ELSEVIER

11 November 1996

PHYSICS LETTERS A

Physics Letters A 222 (1996) 349-353

Photonic band gaps in 3D ordered fcc silica matrices

V.N. Astratov [a], Yu.A. Vlasov [a], O.Z. Karimov [a], A.A. Kaplyanskii [a], Yu.G. Musikhin [b], N.A. Bert [b], V.N. Bogomolov [c], A.V. Prokofiev [c]

[a] *Solid State Physics Department, A.F. Ioffe Physical-Technical Institute, 194021 St. Petersburg, Russian Federation*
[b] *Heterostructures Physics Department, A.F. Ioffe Physical-Technical Institute, 194021 St. Petersburg, Russian Federation*
[c] *Anisotropic Materials Laboratory, A.F. Ioffe Physical-Technical Institute, 194021 St. Petersburg, Russian Federation*

Received 16 August 1996; accepted for publication 26 August 1996
Communicated by V.M. Agranovich

Abstract

The photonic band structure of 3D ordered silica matrices was studied by optical transmission measurements. A decrease of the light attenuation length within the forbidden gap was observed after filling of the opal pores with CdS microcrystals. The parameters of a photonic lattice required for a depletion of the photonic density of states were estimated.

PACS: 42.70.Qs; 81.05.Zx; 42.25.-p; 78.66.Hf

1. Introduction

There has been a growing interest in the fabrication and study of photonic crystals with a 3D periodic modulation of the refractive index, since they possess specific optical properties such as an opening of frequency bands forbidden for light propagation (photonic band gap (PBG) materials), which can lead to the development of a new family of optoelectronic devices (for a recent review see Ref. [1]). Recently we pointed out that synthesized porous silica matrices (synthetic opals) have a highly ordered 3D structure with a period about the wavelength of visible light that permits the study of photonic band gaps at optical frequencies [2]. In that paper the results of the transmission electron microscopy (TEM) characterization of the opals' photonic lattice are presented along with results of spectroscopic studies of their photonic band structure.

2. Samples

The samples of synthetic opals used in this study were fabricated by three subsequent technological procedures. First the monodisperse (standard deviation is less than 5%) suspension of spheres of amorphous SiO_2 were obtained from sol produced by hydrolysis of organic ester of orthosilicic acid in alcohol [3]. The diameter of the spheres can be technologically varied from 0.1 to 0.3 μm. The 3D-periodic structure appeared during settling of the spheres accompanied by their ordering. Finally the sediment was annealed in air and at hydrothermal conditions in autoclave to provide the hardness and to obtain self-supporting solid samples with dimensions of several cm. To modify the refractive index contrast of opal the net of interconnecting empty pores between the spheres can be filled with CdS microcrystals using vapor phase synthesis [2] or with various liquids.

PII S0375-9601(96)00669-X

3. TEM characterization of the photonic lattice

A systematic theoretical search for the structures that possess photonic band gaps have shown that opening up of the PBG is governed by several critical conditions: symmetry of the photonic lattice, long-range order conservation of the "atoms" packaging in all three dimensions, optimal volume packing fraction of the "atoms" and a large enough refractive index contrast between the "atoms" and the surrounding media [1]. In the present study we applied transmission electron microscopy (TEM) for a direct investigation of these parameters in synthetic opals. For the TEM characterization several small pieces were broken along different sample faces and were thinned by a mechanical treatment followed by Ar^+-ion milling to a thickness of several μm. The TEM images were obtained in a bright field mode using a Philips EM420 microscope operating at 100–120 kV.

(a) *Long-range order.* In contrast to natural precious opals composed from μm scale areas of a regular spheres package misoriented from each other [5] the samples of synthetic opals were shown to possess a highly ordered structure in the cm range and can be referred to as single "crystals" rather than "polycrystals". On the TEM micrographs (see Figs. 1a, 1c) taken from the orthogonal faces of one of the samples (sample V13) the regular lattice of spheres can be clearly seen, which demonstrates the existence of ordering in all three dimensions. The conservation of the period and orientation of the sample lattice was controlled by TEM scanning of the areas of about 100 μm^2 in different testing regions. The total inplane density of structural defects (stacking faults, dislocations and point defects) was found to be about 10^7 cm^{-2} or 1 defect per 100 unit cells.

(b) *Symmetry of the lattice.* In general the ordered structures produced from the suspensions of submicron particles can possess both fcc and hcp types of close-packed lattices [6]. The TEM micrograph (Fig. 1a) of the growth plane of the sample displays a characteristic hexagonal sphere packaging in several monolayer-step terraces. The analysis of the positions occupied by the spheres in three subsequent monolayers (see the graphical sketch of spheres packaging in Fig. 1b) revealed the ABCABC... sequence of the layers corresponding to the $\langle 111 \rangle$ direction of the fcc lattice. The TEM micrograph taken from the perpendicular face of the same sample (Fig. 1c) reveals a classical type of spheres packaging on the fcc plane (110) that made it possible to identify the orientation of photonic lattice of the sample.

(c) *Volume packing fraction of the spheres.* The volume packing fraction of the spheres β in synthetic opals is higher than the close-packed value 0.74 as a result of spheres penetration into each other at the stage of annealing. The TEM study showed that the volume packing fraction can be varied from 0.76 (for Figs. 1a, 1c) to unity with a corresponding reduction of the lattice period.

4. Optical studies of synthetic opals

The optical transmission and reflection spectra were taken with a highly parallel incident light beam (divergence less than 1°). The detection of the transmitted and reflected beams was performed within a very narrow angular cone (about 30′) defined by a small aperture lens to minimize the contribution of the diffusely scattered background. All the transmission spectra are presented in a semilog scale. The attenuation is plotted in units of cm^{-1} of the reciprocal attenuation length $l^{-1} = \ln(I/I_0)/d$, where d is the sample thickness.

4.1. Mapping of photonic zones

In our previous experiments the dispersion of photonic zones was studied by changing the angle of light incidence in optical transmission measurements [2]. The results indicated qualitatively the "semi-metallic" type of photonic band structure, namely the energetic overlap of the photonic valence and conduction bands in different sections of the Brillouin zone. However, the quantitative mapping of the photonic band structure by the study of the transmission at oblique incidence encountered serious difficulties because the normal component of the wave-vector is not conserved, which impedes the determination of the wave-vector direction.

In Ref. [2] the dispersion of photonic zones was studied by the optical transmission measurements undertaken at normal incidence to different faces of samples with known orientation of the photonic lattice. The transmission spectrum of the sample V13 (fcc unit cell length a = 297 nm, volume packing fraction

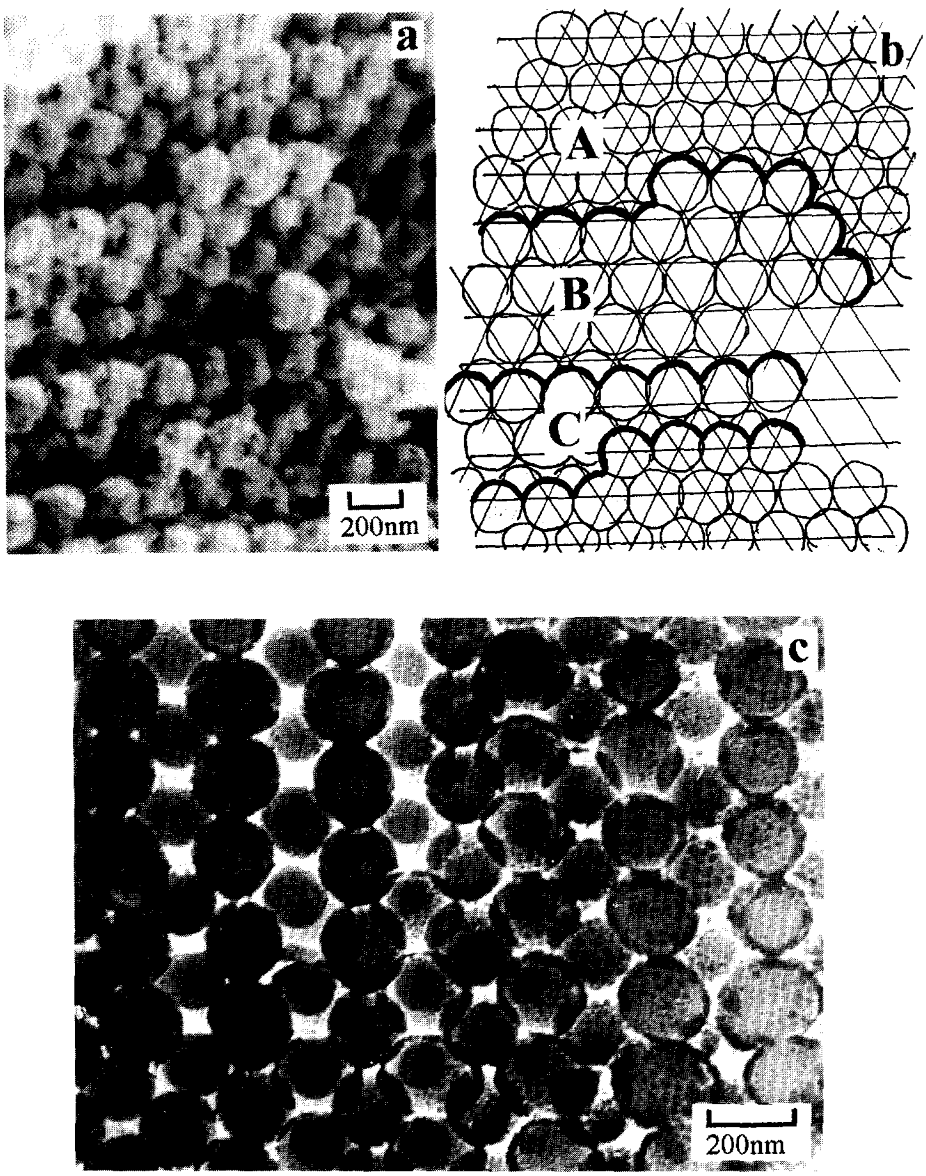

Fig. 1. TEM images of orthogonal faces of the sample V13: (a) (111) plane and (c) (110) plane. (b) Sketch of spheres packaging for TEM image (a).

of the spheres $\beta = 0.76$) taken at normal incidence on the (111) plane is presented in Fig. 2. Two well pronounced drops centered approximately at 2.2 eV and 3.9 eV can be clearly seen within the region of transparency of the silica. These drops can be ascribed to the first and second order Bragg diffraction on the periodic structure considering the interplane spacing $d_{111} = 170$ nm. The light waves from these drops are reflected from the media – compare the reflection spectrum in Fig. 3a with the first order drop in transmission in Fig. 3b. Thus this band can be referred to as the forbidden photonic gap for the $\langle 111 \rangle$ direction of

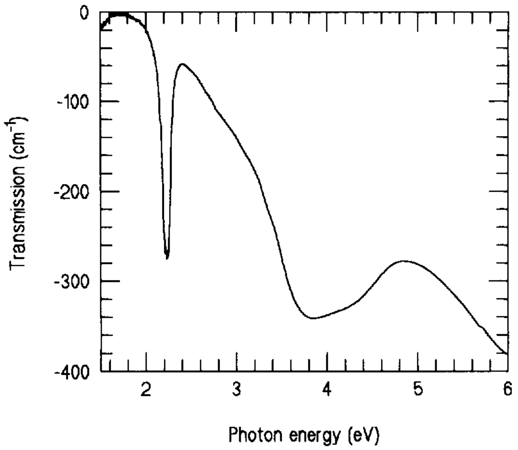

Fig. 2. Transmission spectra of the sample V13 taken at normal incidence to the (111) plane.

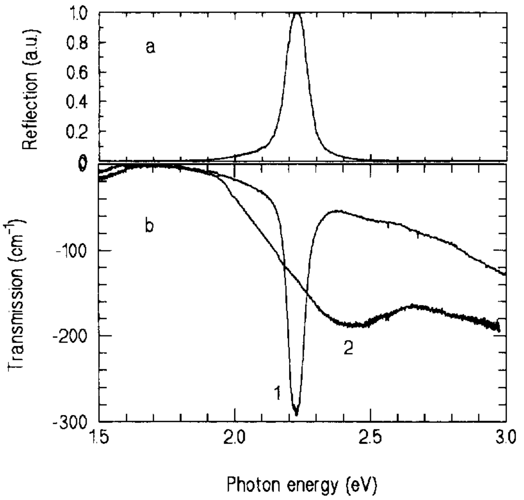

Fig. 3. (a) Reflection spectrum of the sample V13 taken at normal incidence to the (111) plane; (b) Transmission spectra of the sample V13 taken at normal incidence to the (111) plane (spectrum 1) and to the (110) plane (spectrum 2).

propagation. The valence (VB) and conduction (CB) photonic band edges can be defined from spectrum 1 in Fig. 3b as energies where the transmission is cut off (2.15 eV) and rises up again (2.3 eV) respectively. These VB and CB bands edges correspond to the L point at the surface of the fcc Brillouin zone since the direction of the wave-vector is conserved for the normal incidence geometry. The transmission spectrum 2 in Fig. 3b taken at normal incidence on the (110)

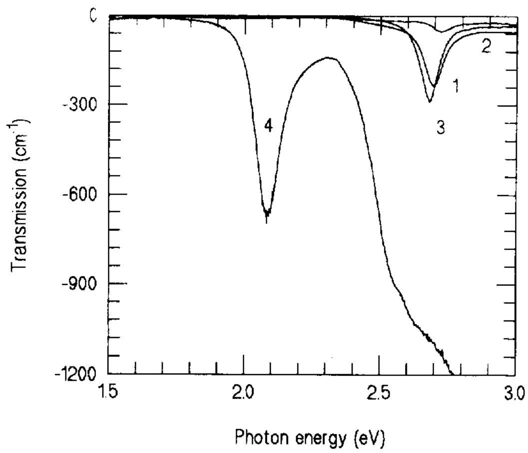

Fig. 4. Transmission spectra of the sample V18 filled with water solutions of α-bromnaphthalene with different refractive indices ((1) $n_b = 1.33$, (2) $n_b = 1.37$, (3) $n_b = 1.47$) and of sample V21 filled with CdS (4).

plane of the sample (point K of the Brillouin zone) shows the shift of the forbidden gap to higher energies (midgap at 2.4 eV). This result can be explained by an about 20% larger value of the wave-vector to the point K in comparison with that to L.

4.2. Refractive index contrast modulation

In order to change the refractive index contrast between the spheres (n_a) and surrounding media (n_b) the pores were filled with water solutions of α-bromnaphthalene ($1.33 \leqslant n_b \leqslant 1.67$). The transmission spectra measured at normal incidence on the (111) plane of the filled opal sample V18 ($a = 260$ nm, $\beta = 0.78$) are presented in Fig. 4 for the cases of $n_b = 1.33$ (spectrum 1), $n_b = 1.37$ (spectrum 2) and $n_b = 1.47$ (spectrum 3) exhibiting the gap in the vicinity of 2.7 eV. It can be seen that the attenuation at the center of the gap dramatically decreases at $n_b = 1.37$ (see spectrum 2). Within the forbidden gap the wave-vector is purely imaginary and the wave decays exponentially. The attenuation length (l) at $n_b = 1.37$ reaches 310 μm and falls down when n_b deviates from this value (for $n_b = 1.33$, $l = 43$ μm and for $n_b = 1.47$ the $l = 35$ μm) which means that the medium approaches optical homogeneity at $n_b \approx 1.37$. This result leads to an estimate of the refractive index of the spheres as $n_a \approx 1.37$.

To increase the refractive index contrast, the pores were filled with CdS by vapor phase synthesis. The heating of the sample during synthesis was accompanied by a penetration of the silica spheres into each other and by an increase of β. The transmission spectrum of the opal sample V21 filled with CdS ($a = 294$ nm, $\beta = 0.96$) measured at normal incidence to the (111) plane is presented in Fig. 4, spectrum 4. At energies higher than the bulk absorption edge (2.5 eV at 300 K) a clearly seen decrease of transmission is defined by the absorption of light in the semiconductor that fills each of the pores as an aggregate of individual nanocrystals [2]. Below the absorption edge, the photonic forbidden gap can be seen at 2.1 eV. In order to study changes of l induced by impregnation of the pores with CdS a reference piece was broken from the same V21 sample before the semiconductor synthesis and then it was annealed at the identical temperature conditions to provide the same β value. The comparison of transmission data obtained on the reference sample and on the opal/CdS sample showed that the filling of the pores with the semiconductor is accompanied by a decrease of l at the midgap from 30 μm to 15 μm, i.e. to about only 90 lattice planes along the $\langle 111 \rangle$ direction. It should be noted that the value of l observed in the fabricated opal/CdS system is also essentially smaller than in opal filled with liquids (see spectra 1–4 in Fig. 4) indicating the larger perturbation of photonic states caused by enhanced Bragg scattering.

It has been shown theoretically [4] that the parameter ε_r (relative fluctuation of dielectric permittivity from its spatial average) provides a measure of the deviation of photon behavior in strongly scattering media from the free photon case. Hence the increase of ε_r should correspond to the decrease of l. Indeed for the case $n_b = 1.33$ (corresponding to spectrum 1 on Fig. 4) the calculated value $\varepsilon_r = 0.03$ is smaller than $\varepsilon_r = 0.06$ for $n_b = 1.47$ (spectrum 3). The estimation of ε_r for opal/CdS under the assumption of complete filling of the pore volume with the semiconductor ($n_b = 2.5$) gives the value of $\varepsilon_r = 0.4$, which can explain the dramatic decrease of l observed in this case.

It is known [4] that for an fcc lattice with spherical "atoms", to which the opal structure belongs, the total suppression of a density of photonic states (complete PBG) can be achieved only in the highest order forbidden gaps. Due to symmetry restrictions the lowest-lying zones possess a "semimetallic" structure that prevents the first order PBG to open up. However the very large depletion of the photonic density of states (so-called "pseudogap") can be achieved under appropriate structural parameters (volume packing fraction and refractive index contrast) [7]. It has been demonstrated that $\varepsilon_r \sim 1$ is the point where the "pseudogaps", or complete PBGs (if they are allowed by symmetry), begin to emerge [4]. Taking into account the really attainable β in the opal structure ($0.74 < \beta < 1$), it can be shown that the "air spheres" type of lattice ($n_a < n_b$) is more favorable for maximizing the ε_r than the "dielectic spheres" type ($n_a > n_b$). In the case of filling of the opal pores with a semiconductor it is the "air spheres" type of lattice that is realized. Our estimations show that in this case the criterion for a low-lying "pseudogap" or highest in energy complete PBG for the opal lattice with $\beta \approx 0.9$ is $n_b \geqslant 3.3$, which can be achieved by the filling of the pores with such semiconductors like ZnTe, GaAs, Ge, Si, etc.

Acknowledgement

We gratefully acknowledge partial financial support from the Russian Foundation for Fundamental Studies (grants 960217928 and 960217931) and from the State Program "Physics of Solid Nanostructures" (1-061/3).

References

[1] Special issue of J. Opt. Soc. Am. B 10 (1993) pp. 280–408.
[2] V.N. Astratov, V.N. Bogomolov, A.A. Kaplyanskii, A.V. Prokofiev, L.A. Samoilovich, S.M. Samoilovich and Yu.A. Vlasov, Nuovo Cimento D 17 (1995) 1349; in: Highlights of light spectroscopy on semiconductors, ed. A. D'Andrea (World Scientific, Singapore, 1995).
[3] V.G. Balakirev et al., Kristalografia 38 (1993) 348.
[4] H.S. Sözuer, J.W. Haus and R. Inguva, Phys. Rev. B 45 (1992) 13962.
[5] J.V. Sanders, Acta Cryst. A 24 (1968) 427; Nature 204, no. 4964 (1964) 1151.
[6] P.C. Ohara, D.V. Leff, J.R. Heath and W.M. Gelbart, Phys. Rev. Lett. 75 (1995) 3466.
[7] Z. Zhang and S. Satpathy, Phys. Rev. Lett. 65 (1990) 2650.